

Mineral elements and toxicants

UDC 636.085.12:636.087.72

doi: 10.15389/agrobiol.2023.6.1122eng
doi: 10.15389/agrobiol.2023.6.1122rus

BACTERIAL LUMINESCENCE OF MANGANESE- AND COBALT-CONTAINING ULTRAFINE PARTICLES (Mn_2O_3 and Co_3O_4) IN THE RUMEN FLUID

D.E. SHOSHIN^{1, 2} ✉, E.A. SIZOVA^{1, 2}, A.M. KAMIROVA¹

¹Federal Research Centre of Biological Systems and Agrotechnologies RAS, 29, ul. 9 Yanvarya, Orenburg, 460000, e-mail daniilshoshin@mail.ru (✉ corresponding author), sizova.178@yandex.ru, ayna.makaeva@mail.ru;

²Orenburg State University, 13, prosp. Pobedy, Orenburg, 460018 Russia

ORCID:

Shoshin D.E. orcid.org/0000-0003-3086-681X

Kamirova A.M. orcid.org/0000-0003-1474-8223

Sizova E.A. orcid.org/0000-0002-5125-5981

The authors declare no conflict of interests

Acknowledgements:

Supported financially by the Russian Science Foundation (project No. 22-26-00254)

Final revision received June 05, 2023

Accepted July 12, 2023

Abstract

Along with the main nutrients, proteins, fats and carbohydrates, mineral elements are important in feeding farm animals, including cattle and poultry (D.V. Mashnin et al., 2022; T.M. Okolelova et al., 2018). Their inorganic or organic forms are components of premixes (M.Y. Mishanin et al., 2021; O.S. Koschaeva 2018). However, nanocompositions are more promising, the properties of which can be modeled by changing the shape, synthesis paths and size of ultrafine particles (UFP) (S. Miroshnikov et al., 2019). However, the use of UFPs has a number of limitations related to their potential toxicity (E. Rusakova et al., 2015). It is also known that the symbiotic microflora forms a multicomponent suspension of organic substances, intermediate and final metabolites of the microbiome, capable of interacting with UFP (B.S. Nurzhanov et al., 2019). In this work, the dynamics of luminescence of a bacterial test object was established for the first time when a complex of UFPs and rumen fluid was introduced into the nutrient medium. This combination has been shown to neutralize the toxicity of nano-structures. The purpose of our work was to evaluate the properties of ultrafine particles using the example of various concentrations of manganese and cobalt oxide in the biochemical environment of the ruminal community based on the method of inhibition of bacterial luminescence. The study was conducted on the basis of the center Nanotechnology in Agriculture of the FRC BST RAS (Orenburg) in 2022. Chemically pure manganese oxides Mn_2O_3 and cobalt Co_3O_4 (99 %) for analysis in the amount of 157.8 and 240.7 mg were dispersed by ultrasound at a frequency of 35 kHz in 1 ml of distilled water for 30 minutes at 25 °C. The rumen fluid (RF) was collected through a chronic rumen fistula (d = 80 mm, ANKOM Technology Corporation, USA) 3 hours after feeding in a Kazakh white-headed bull, whose main diet was 30 % concentrates and 70 % coarse feed without the addition of UFP. The luminescent bacterial test Ecolum (a lyophilized culture of *Escherichia coli* microorganisms carrying a hybrid plasmid pUC19 with *luxCDABE* cloned *P. leiognathi* 54D10 genes, SIS IMMUNOTECH, Russia) was used. In a bioluminescent plan, a series of double dilutions of the UFP and RF suspension was prepared starting from 50 μ l Mn_2O_3 (1 mol/l) + 50 μ l RF; 50 μ l Co_3O_4 (1 mol/l) + 50 μ l RF; 50 μ l Mn_2O_3 (1 mol/l) + 50 μ l distilled water; 50 μ l Co_3O_4 (1 mol/l) + 50 μ l distilled water; 100 μ l RF; 100 μ l distilled water (control). Then 100 μ l of the Ecolume test system were added to each cell to a total concentrations of UFPs from 0.25 to 0.00025 mol/l and dilution of RF from 1_2 to 1:2048 in a pure test and from 1:4 to 1:4096 in the test with UFPs. The toxicity of the studied samples was determined on a multifunctional micro-lancet reader TECAN Infinite F200 (Tecan Austria GmbH, Austria), fixing the luminescence value of the bacterial strain *E. coli* K12 TG1 at different concentrations of ultrafine particles and rumen fluid for 3 hours with a period of 5 minutes. Based on the obtained data, graphs reflecting the dynamics of bioluminescence inhibition were constructed and the toxicity index (T) and the relative value of bioluminescence (A) was calculated. It was found that UFPs in their pure form cause dose-dependent inhibition of bacterial luminescence, suppressing over 50 % of the luminescence (EC_{50}) even when diluted by 2048 times (0.00025 mol/l). The values of the toxicity index, when calculating which the control is taken as 100 %, clearly indicate a decrease in the toxic properties of suspensions with a decrease in the proportion of UFPs in them. For

Mn₂O₃, this value ranged from 89.76 % at a concentration of 0.25 mol/l to 38.57 % at 0.00025 mol/l at the 1st minute of the exposure and from 95.16 to 52.85 % at the end of the 3rd hour; for Co₃O₄ — 99.44 and 32.80 %, respectively, at the 1st minute, and 99.43 and 54.72 % at the end of the 3rd hour. Similar indicators in the experiment with rumen fluid appeared only in the first minutes of exposure, after which the luminosity increased significantly, reaching 769.10 % to the control at 64-fold dilution. When combining rumen fluid with UFPs, a regression of the toxic properties of the latter was observed, although the maximum luminosity in combination with Mn₂O₃ was only 43.28 % of those for native RF, in combination with Co₃O₄ 36.44 %. The observed changes in luminescence were divided into three types. The first type is control (luminescence changes in proportion to the growth phases of the bacterial culture; without additives). The second type corresponds to deep changes (suppression of luminescence throughout the entire exposure period; with the addition of UFPs), and the third type is competitive (increase in luminescence from the beginning to the end of the experiment; with the addition of RF or a complex of RF+UFP). Thus, the combination of rumen fluid with metal oxide particles leads to an inhibition of their toxicity to the test object.

Keywords: ultrafine particles, bacterial cells, bioluminescence, manganese oxide, cobalt oxide, rumen fluid

Along with proteins, fats and carbohydrates as the main nutrients, mineral elements are important in feeding farm animals, including cattle and poultry [1, 2]. Mineral elements are components of accessory substances, e.g., respiratory pigments, vitamins, hormones, enzymes and coenzymes, and influence a variety of physiological processes which affects growth and ontogeny [3, 4]. Optimal supply of microelements with feed is a factor mediating high animal productivity performance [5, 6]. Therefore, improving various formulants of mineral-containing premixes is relevant.

Traditionally, inorganic and organic compounds are used in premixes [7, 8], but chelates and nanoforms of essential elements are more promising [9-11]. The properties of the latter can be modeled by changing the shape, synthetic reactions and particle size [12]. However, this cheaper and highly cost-effective method of fortifying feed with micronutrients [13, 14] has some limitations. Ultrafine particles (UFPs) impose risks of potential toxicity [15]. Thus, though stable metal oxides are absolutely inert, metal UFPs with redox potential can be genotoxic and cytotoxic [16] due to high bioavailability, a synergistic effect with other pollutants that may occur [17] and wide variability of properties depending on the nature, size, concentration, ζ -potential, shape and reaction medium.

The latter is especially relevant for ruminants, in which the ruminal contents, in fact, is an integral ecosystem with many connections [18]. Symbiotic microbiota also needs macro- and microelements to maintain normal metabolism and produces a multicomponent suspension of organic substances, the intermediate and final metabolites of the microbiome that can interact with UFPs [19]. This should be accounted when determining the maximum permissible doses of dietary UFPs for animals.

This work is the first report on the pattern of *in vivo* luminescence bacterium test when a UFP complex and rumen fluid were added to the nutrient medium. It has been shown that this combination neutralizes the toxicity of nanostructures.

Our goal was to evaluate the properties of ultrafine particles using the example of different concentrations of manganese and cobalt oxide in the biochemical environment of the ruminal community based on the method of inhibiting bacterial luminescence.

Materials and methods. The study was carried out in 2022 (the Federal Scientific Center BST RAS, the Center Nanotechnologies in Agriculture, Orenburg). UFPs of manganese oxide Mn₂O₃ and cobalt oxide Co₃O₄ chemically pure for analysis (grade 99%, IP Khisamutdinov R.A., Russia) were used (157.8 and 240.7 mg. respectively; laboratory scales VLA-225M, accuracy class I, permissible error ± 0.5 mg, Gosmetr, Russia). Oxides were ultrasonically dispersed by

(35 kHz) in 1 ml of distilled water for 30 min at 25 °C.

Three hours after feeding, rumen fluid (RF) was collected through a chronic rumen fistula (d = 80 mm, ANKOM Technology Corporation, USA) of a Kazakh white-headed bull (250 kg weight, 10 month age). The basal diet was 30% concentrates and 70% roughage without the addition of UFPs. RF was delivered within 30 min at 38.5-39.5 °C. Before use, the RF was thoroughly shaken and filtered.

The luminescent bacterial test Ecolum (NVO IMMUNOTECH, Russia), consisting of a lyophilized *Escherichia coli* carrying the hybrid plasmid pUC19 with the cloned *luxCDABE* genes of *P. leiognathi* 54D10, was prepared according to the method by E.S. Aleshina et al. [20]. Distilled water cooled to 4 °C (10 ml) was added to the strain, and the suspension was allowed for 30 min at the same temperature.

Serial two-fold dilutions were performed in a bioluminescent plate. The starting samples were as follows: 50 µl Mn₂O₃ (1 mol/l) + 50 µl RF for line A, 50 µl Co₃O₄ (1 mol/l) + 50 µl RF for line B, 50 µl Mn₂O₃ (1 mol/l) + 50 µl distilled water for line C, 50 µl Co₃O₄ (1 mol/l) + 50 µl distilled water for line D; 100 µl RF for line E, 100 µl distilled water for line F (control). To each cell, 100 µl of the Ecolum test system was added to final UFPs concentrations from 0.25 to 0.00025 mol/l and RF dilutions from 1:2 to 1:2048 in the test without UFPs and from 1:4 to 1:4096 with UFPs.

The toxicity of the samples was determined (a multifunctional microplate reader TECAN Infinite F200, Tecan Austria GmbH, Austria), recording the luminescence of the bacterial strain *E. coli* K12 TG1 (Ecolum) in a medium with different concentration of ultrafine particles and rumen fluid during 3 h each 5 min.

Based on these data, graphs were constructed of the dynamics of bioluminescence inhibition, and the toxicity index (T) was calculated:

$$T = (I_c - I_t) / I_c \times 100\%,$$

where I_c is luminosity of the control sample, I_t is the luminosity of the test sample.

This indicator was used to assess how strong the negative impact of the factor under study is. However, if the latter has a positive component and intensifies the luminosity, it is more rational to calculate the relative value of bioluminescence (A) in order to avoid negative values:

$$A = I_c / I_t \times 100\%.$$

In essence, this value is the inverse of the toxicity index, reflecting the difference between the luminescence intensity of the control and test samples.

Statistical processing of the results was carried out using the Statistica 12 software (StatSoft Inc., USA) and Microsoft Excel package (Microsoft, USA). The significance of the differences between the absolute values of luminescence was determined assessed using the Student's *t*-test with the required significance level $p \leq 0.01$. The tables indicate relative values corresponding to this threshold.

Results. Manganese and cobalt, along with other transition metals (Fe, Ni, Cu, Zn), are essential microelements involved in a number of biochemical transformations in bacteria [21, 22], plants [23-25], protozoa [26, 27], invertebrate [28, 29] and vertebrate [30, 31] animals. Specifically, manganese is responsible for macronutrient metabolism, bone formation, free radical defense systems, ammonia clearance, and neurotransmitter synthesis in the brain. It is a cofactor for enzymes that degrade reactive oxygen species, mainly Mn-superoxide dismutase (SOD) and Mn-cofactored catalases and peroxidase [32, 33]. In addition, Mn replaces iron in some Fe-mononuclear enzymes in *E. coli* under oxidative stress, protecting them from Fenton reaction-mediated oxidative damage while main-

taining catalytic activity [34, 35]. To maintain optimal concentrations of metal ions, bacteria use molecular importers and exporters [36, 37].

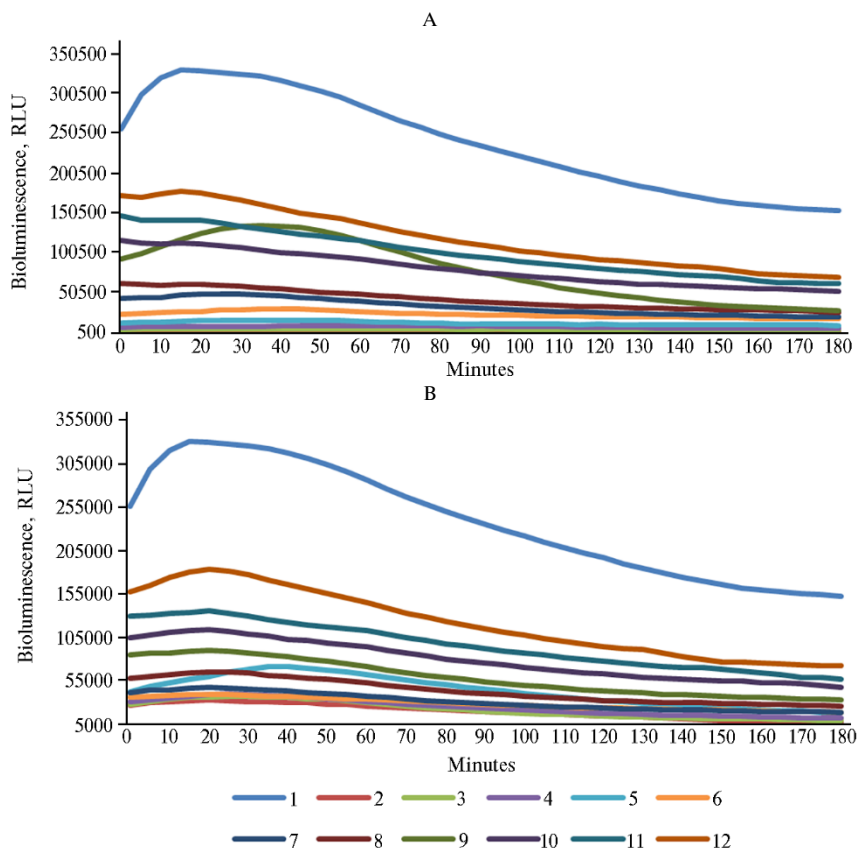


Fig. 1. Bioluminescence of *Escherichia coli* K12TG1 with a suspension of ultrafine particles (UFPs) Co_3O_4 (A) and Mn_2O_3 (B) depending on concentrations: 1 – 0 mol/l (control), 2 – 0.25 mol/l, 3 – 0.125 mol/l, 4 – 0.063 mol/l, 5 – 0.031 mol/l, 6 – 0.016 mol/l, 7 – 0.008 mol/l, 8 – 0.004 mol/l, 9 – 0.002 mol/l, 10 – 0.001 mol/l, 11 – 0.0005 mol/l, 12 – 0.00025 mol/l.

Mn is essential component in dozens of proteins and enzymes found in all tissues, especially those rich in mitochondria and melanin. Normally, conmaximum Mn concentrations are characteristic of the liver and pancreas [38]. With its excess or deficiency in the diet, neurodegenerative disorders most often occur [39-41].

Cobalt is used by bacteria to synthesize the tetrapyrrole ring known as corrin of vitamin B₁₂ ($\text{C}_{63}\text{H}_{88}\text{O}_{14}\text{N}_{14}\text{PCo}$) [21, 42] the chemical structure and properties of which have been described in detail by D. Osman et al. [43]. Cobalt is involved in nitrogen fixation in plants, serves as a cofactor for adenosylcobalamin-dependent isomerases, ethanolamine ammonia lyase, methylcobalamin-dependent methyltransferase, ribonucleotide reductase, and number of metalloproteins in animals, bacteria and yeast [24]. In humans, Co is a component of ethylmalonyl-CoA mutase (MCM) and methionine synthase the deficiency of which leads to methylmalonic aciduria and megaloblastic anemia [44], neural tube defects, stroke and dementia, and retarded intellectual development in children [45]. In excess, Co has genotoxic and carcinogenic properties [46].

The bioluminescence of samples with different UFP concentrations of manganese and cobalt oxides without RF was inversely proportional to their concentration (Fig. 1). At the beginning of the experiment, the luminosity of the

control sample due to intensive consumption of the nutrient substrate increased by 22.5% in 15 min and then gradually decreased to 59.6% of the initial value. At the largest dilution of 0.00025 mol/l, the luminosity of Mn₂O₃ and Co₃O₄ suspensions vs. the control sample in the first second was 61.4 and 67.2%, respectively, whereas at 0.25 mol/l dilution only 10.2 and 0.5%.

1. Toxicity index (T, %) of different concentrations of Co₃O₄ ultrafine particles (UFPs) suspensions at assessed by co-exposition with the luminescent strain *Escherichia coli* K12TG1 in distilled water

Minutes	UFP concentration, mol×10 ⁻³ /l										
	250	125	63	31	16	8	4	2	1	0.5	0.25
0	99.4/A	99.0/A	97.8/A	95.6/A	91.5/A	83.5/A	76.1/A	64.0/B	54.8/B	43.0/C	32.8/C
30	99.7/A	99.0/A	97.8/A	95.5/A	91.3/A	85.3/A	82.3/A	59.1/B	67.2/B	58.9/B	49.0/C
60	99.7/A	99.0/A	97.3/A	95.3/A	91.0/A	86.5/A	83.5/A	59.8/B	67.9/B	59.7/B	51.8/B
90	99.7/A	98.8/A	96.9/A	95.6/A	90.8/A	87.4/A	84.0/A	68.0/B	68.2/B	60.1/B	53.4/B
120	99.6/A	98.6/A	97.1/A	95.2/A	90.3/A	87.4/A	83.7/A	75.1/A	67.5/B	59.6/B	53.6/B
150	99.5/A	98.5/A	97.2/A	94.6/A	89.1/A	87.0/A	83.1/A	79.5/A	65.8/B	57.6/B	51.9/B
180	99.4/A	98.4/A	97.3/A	94.6/A	89.3/A	87.8/A	83.8/A	82.7/A	66.7/B	60.2/B	54.7/B

Note. A — EC₇₀, B — EC₅₀, C — EC₂₀, that is, UFP concentrations that cause over 75, 50 and 20% quenching of the biosensor compared to the control.

The values of the T index to calculate which we take the control as 100%, clearly indicate a decrease in the toxic properties of the suspension with a decrease in the UFP concentration. For Mn₂O₃, the T value ranged from 89.76% at 0.25 mol/l to 38.57% at 0.00025 mol/l during the 1st minute of the exposition and from 95.16 to 52.85% at the end of the 3rd hour of the exposition (Table 1). For Co₃O₄, the T index was 99.44 and 32.80% at the 1st minute and 99.43 and 54.72% at the end of the 3rd hour (Table 2).

2. Toxicity index (T, %) of different concentrations of Mn₂O₃ ultrafine particles (UFPs) suspensions assessed by co-exposition with the luminescent strain *Escherichia coli* K12TG1 in distilled water

Minutes	UFP concentration, mol×10 ⁻³ /l										
	250	125	63	31	16	8	4	2	1	0.5	0.25
0	89.8/A	89.0/A	87.9/A	83.7/A	85.9/A	83.8/A	77.3/A	66.7/B	59.0/B	49.3/B	38.6/C
30	90.4/A	88.7/A	88.0/A	79.0/A	88.3/A	86.1/A	80.5/A	73.3/B	66.4/B	60.2/B	45.5/B
60	91.0/A	89.6/A	89.1/A	78.5/A	88.2/A	86.9/A	81.7/A	75.0/B	67.1/B	60.7/B	49.4/B
90	91.7/A	91.6/A	90.1/A	80.9/A	88.3/A	87.7/A	83.1/A	77.0/A	68.1/B	61.0/B	51.0/B
120	92.5/A	92.7/A	91.0/A	83.7/A	88.1/A	88.0/A	83.6/A	78.0/A	68.1/B	60.7/B	52.2/B
150	94.3/A	93.4/A	91.3/A	86.0/A	87.4/A	87.4/A	82.6/A	77.5/A	66.8/B	59.0/B	53.6/B
180	95.2/A	94.0/A	92.1/A	88.3/A	87.8/A	87.9/A	83.4/A	78.5/A	68.8/B	62.5/B	52.9/B

Note. A — EC₇₀, B — EC₅₀, C — EC₂₀, that is, UFP concentrations that cause over 75, 50 and 20% quenching of the biosensor compared to the control.

In the test with ruminal fluid without UFPs, the relative bioluminescence ranged from 25.29 to 769.10% with a tendency to increase. Thus, the first test with RF during the first 30 min showed EC₇₀ and EC₃₀, that is, inhibition of 70 and 30% of the luminescence of the luminescent strain, respectively. However, starting from the 2nd hour, the sample could not be assessed as toxic; moreover, its indicators by the end of the experiment were 3.5 times higher than the control (Fig. 2). In the dilution 1:4, the intensity of bioluminescence in the first second corresponded to the EC₅₀ and then increased 6.8 times, or 5.27 times compared to control. In general, the luminosity of the samples was inversely proportional to the concentration of rumen fluid up to 1:32-1:64 dilutions after which the trend changed. Moreover, within one concentration, the bioluminescence increased within 3 hours until the 1:128 dilution, then (1:256-1:2048) in the first 30 min an increase in bioluminescence was recorded followed by a drop below the initial level. The overall dynamics demonstrated a sharp increase in biolu-

minescence in the first 20-30 min followed by a slowdown (for 4-128-fold dilutions) or a slow decrease in the bioluminescence intensity (for 256-2048-fold dilutions) (Table 3).

When rumen fluid was co-incubated with ultrafine particles of manganese and cobalt oxides, the toxic properties of the latter regressed. As a result, the graphs of bioluminescence dynamics approached that of rumen fluid (Fig. 3), although the maximum luminescence in combination with Mn_2O_3 were only 43.28% of that for native RF, with Co_3O_4 36.44%. For Mn_2O_3 , samples with UFP concentrations of 0.00025 and 0.0005 mol/l followed the changes in the control, but exceeded in the luminescence level. All other samples were initially inferior in bioluminescence to the suspension without UFPs, but overtook it at various time intervals, exceeding by 2.32-3.22 times at the end of the test. For Co_3O_4 , the dynamics were the same as in the control, but luminescence did not exceed the values of the sample with UFP concentrations of 0.004 and 0.002 mol/l. On the contrary, dilutions of 0.001-0.0002 mol/l, having the same dynamics, exceeded the control values, 0.25-0.031 mol/l did not reach them, and 0.016 and 0.008 mol/l exceeded them by only 1.14-1.55 times.

3. Relative bioluminescence (A, %) depending on the dilution of a Kazakh white-headed bull ruminal fluid (RF) assessed by co-exposition with the luminescent strain *Escherichia coli* K12TG1

Minutes	RF dilutions											
	1:2	1:4	1:8	1:16	1:32	1:64	1:128	1:256	1:512	1:1024	1:2048	
0	25.2/A	45.9/B	75.19/C	91.3/D	118.4/E	138.1/E	134.4/E	132.0/E	130.7/E	121.1/E	118.7/E	
30	69.6/C	126.9/E	189.3/E	207.7/E	228.4/E	232.2/E	207.3/E	191.3/E	179.9/E	178.6/E	145.8/E	
60	98.5/D	160.7/E	235.2/E	269.6/E	298.6/E	292.2/E	237.0/E	206.4/E	184.3/E	178.4/E	144.3/E	
90	140.6/E	208.6/E	303.3/E	366.0/E	369.0/E	366.7/E	264.6/E	224.4/E	187.4/E	177.9/E	136.9/E	
120	233.4/E	294.9/E	397.5/E	459.8/E	453.8/E	459.8/E	300.4/E	226.0/E	176.7/E	167.5/E	128.2/E	
150	309.6/E	423.41/E	491.7/E	538.0/E	592.6/E	622.1/E	324.9/E	216.6/E	160.1/E	156.4/E	124.6/E	
180	368.7/E	526.73/E	603.2/E	636.7/E	670.1/E	769.1/E	349.8/E	193.7/E	139.0/E	144.2/E	117.2/E	

Note. A — EC70, B — EC50, B — EC20, B — NTOX, E — NTOX+, that is, UFP concentrations that cause over 75, 50 and 20% quenching of the biosensor compared to the control, non-toxic and luminescence-intensifying concentrations.

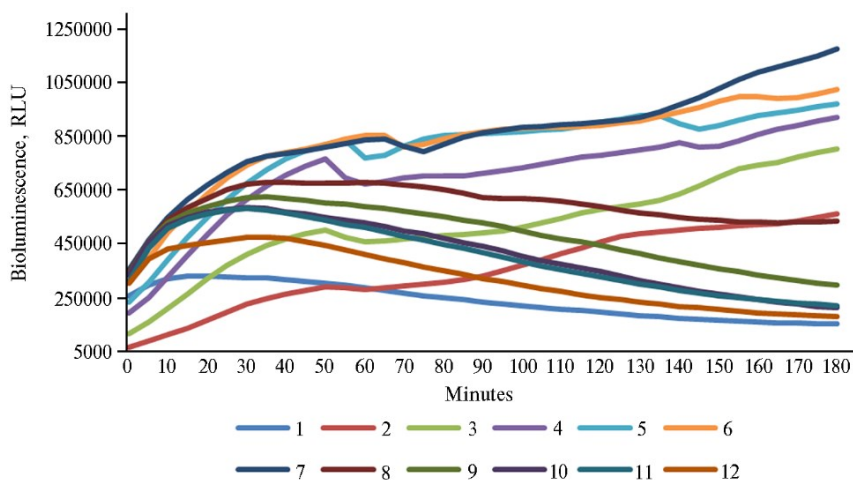


Fig. 2. Bioluminescence of *Escherichia coli* K12TG1 in the rumen fluid of a Kazakh white-headed bull depending on the dilution: 1 — control (distilled water), 2 — 2-fold, 3 — 4-fold, 4 — 8-fold, 5 — 16-fold, 6 — 32-fold, 7 — 64-fold, 8 — 128-fold, 9 — 256-fold, 10 — 512-fold, 11 — 1024-fold, 12 — 2048-fold.

These data indicate the greater toxicity of cobalt oxide compared to manganese oxide. Calculated relative bioluminescence parameters confirmed the con-

clusion (Tables 4, 5). In general, these data implied UFP subtoxic concentrations which are the amounts that did not cause more than 20% quenching of bioluminescence throughout the entire experiment. For Mn_2O_3 and Co_3O_4 , these were 0.001 mol/l concentrations and a 1024-fold dilution of rumen fluid.

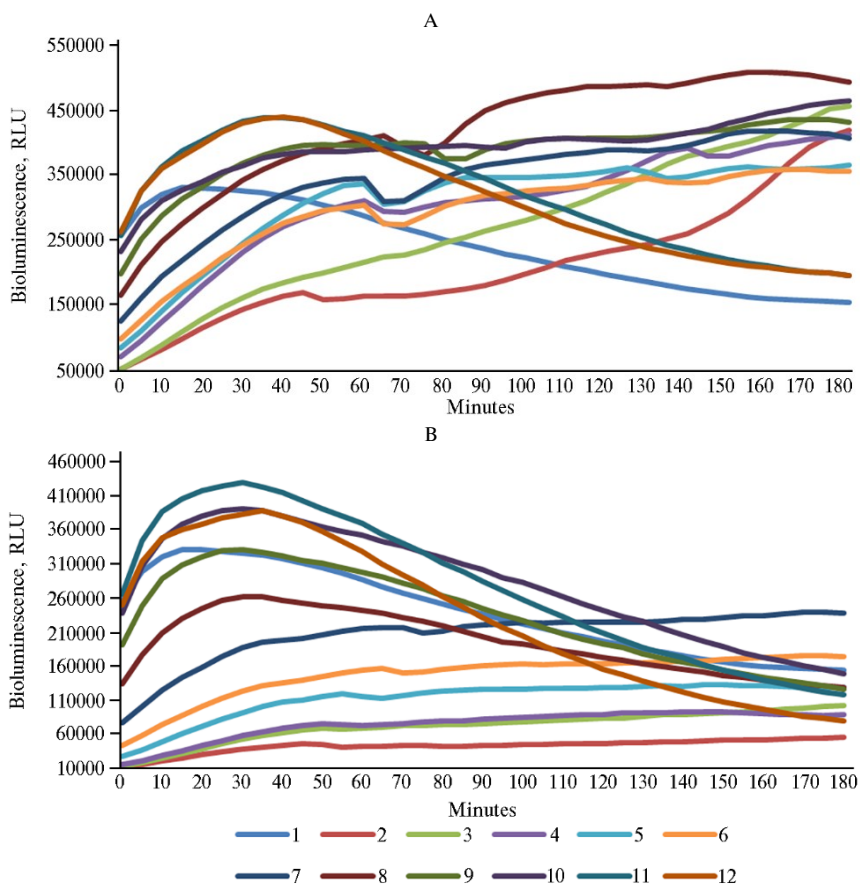


Fig. 3. Bioluminescence of the *Escherichia coli* K12TG1 depending on the dilution of a Kazakh white-headed bull rumen fluid (RF) and UFP Mn_2O_3 (A) and Co_3O_4 (B) concentrations: 1 – 0 mol/l (distilled water, control), 2 – 0.25 mol/l (2-fold dilution), 3 – 0.125 mol/l (4-fold), 4 – 0.063 mol/l (8-fold), 5 – 0.031 mol/l (16-fold), 6 – 0.016 mol/l (32-fold), 7 – 0.008 mol/l (64-fold), 8 – 0.004 mol/l (128-fold), 9 – 0.002 mol/l (256-fold), 10 – 0.001 mol/l (512-fold), 11 – 0.0005 mol/l (1024-fold), 12 – 0.00025 mol/l (2048-fold).

4. Relative bioluminescence (A, %) depending on a Kazakh white-headed bull ruminal fluid (RF) dilutions, Mn_2O_3 ultrafine particles (UFPs) concentrations and the time of co-exposition with the luminescent strain *Escherichia coli* K12TG1

Minutes	UFP concentration, mol $\times 10^{-3}$ /l (RF dilution)										
	250 (1:2)	125 (1:4)	63 (1:8)	31 (1:16)	16 (1:32)	8 (1:64)	4 (1:128)	2 (1:256)	1 (1:512)	0.5 (1:1024)	0.25 (1:2048)
0	19.6/A	19.6/A	27.1/A	32.1/B	37.6/B	48.4/B	64.3/B	77.1/B	90.2/D	99.9/D	102.4/D
30	43.6/B	49.4/B	70.6/C	74.9/C	74.0/C	87.7/D	105.1/D	113.1/D	112.0/D	132.8/E	132.0/E
60	56.8/C	75.2/C	108.3/D	117.4/D	106.0/D	120.5/E	141.0/E	138.0/E	136.0/E	143.3/E	140.6/E
90	76.4/C	111.8/D	132.7/E	146.9/E	135.6/E	154.9/E	191.0/E	165.4/E	166.7/E	146.5/E	137.6/E
120	117.6/D	164.6/E	175.2/E	181.0/E	172.2/E	197.9/E	247.6/E	206.6/E	205.7/E	138.7/E	129.8/E
150	175.5/E	238.0/E	228.8/E	217.7/E	210.1/E	249.6/E	304.7/E	254.2/E	259.6/E	132.6/E	129.3/E
180	273.7/E	298.4/E	269.5/E	238.5/E	232.8/E	265.8/E	322.5/E	281.9/E	304.0/E	127.5/E	127.7/E

Note. A – EC70, B – EC50, C – EC20, D – NTOX, E – NTOX+, that is, UDP concentrations that cause over 75, 50 and 20% quenching of the biosensor compared to the control, non-toxic and luminescence-intensifying concentrations.

5. Relative bioluminescence (A, %) depending on a Kazakh white-headed bull ruminal fluid (RF) dilutions, Co₃O₄ ultrafine particles (UFPs) concentrations and the time of co-exposition with the luminescent strain *Escherichia coli* K12TG1

Minute s	UFP concentration, mol×10 ⁻³ /l (RF dilution)										
	250 (1:2)	125 (1:4)	63 (1:8)	31 (1:16)	16 (1:32)	8 (1:64)	4 (1:128)	2 (1:256)	1 (1:512)	0,5 (1:1024)	0,25 (1:2048)
0	4.5/A	5.0/A	5.9/A	10.3/A	17.0/A	29.5/B	51.9/B	74.5/B	92.8/D	103.7/D	97.1/D
30	11.5/A	16.0/A	17.5/A	27.9/B	37.8/B	57.2/B	80.5/D	101.6/D	120.1/D	131.7/D	117.6/D
60	14.4/A	24.0/B	25.1/B	40.2/B	53.5/B	75.0/B	84.4/D	103.9/D	122.8/D	128.8/D	114.5/D

Continued Table 5

90	18.2/A	32.0/B	34.3/B	53.2/B	68.2/B	93.6/D	86.2/D	103.8/D	127.7/D	120.6/D	98.0/D
120	23.5/B	41.8/B	44.9/B	65.2/B	82.9/D	114.2/D	87.6/D	97.7/D	122.5/D	105.9/D	79.0/B
150	30.6/B	54.9/B	55.5/B	79.5/B	102.3/D	139.1/D	88.1/D	92.8/D	113.6/D	93.1/D	64.6/B
180	35.7/B	66.0/B	57.3/B	83.4/D	113.8/D	155.1/D	83.7/D	82.4/D	97.1/D	76.6/B	51.5/B

Note. A – EC₇₀, B – EC₅₀, C – EC₂₀, D – NTOX, E – NTOX+, that is, UDP concentrations that cause over 75, 50 and 20% quenching of the biosensor compared to the control, non-toxic and luminescence-intensifying concentrations.

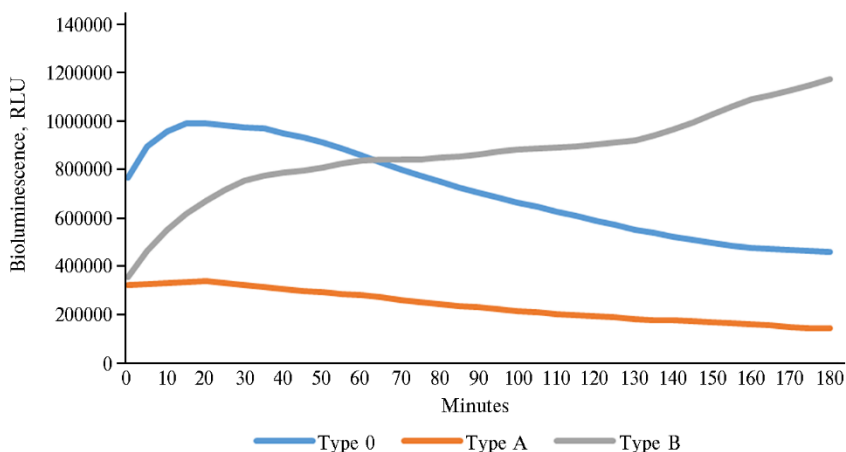


Fig. 4. Bioluminescence of *Escherichia coli* K12TG1 exposed to ruminal fluid (RF), ultrafine particles (UFPs) or RF + UFPs: type 0 – control (luminescence dynamics corresponds to the growth phases of the bacterial culture), type A – deep (extinguishing the glow by ultrafine particles throughout the entire experiment), type B – competitive (luminescence intensifies, changing from negative to positive values as influenced by RF of a Kazakh white-headed bull or a RF + UFPs complex throughout the entire experiment).

According to the data we obtained, all dynamic processes could be divided into several types (Fig. 4).

Type 0 (control) means that in the absence of UFPs and RF in the medium, the luminosity of *E. coli* K12TG1 was proportional to the culture growth rate and corresponded to the phases of logarithmic growth, negative acceleration, stationary phase and death phase. The lag phase and positive acceleration occurred during the sample preparation for analysis.

Type A (deep) means that in the presence of UFPs of manganese and cobalt oxides, the bioluminescence decreased throughout the entire exposure period. This illustrates a deep degenerative effect, the degree of which decreased with the concentration of UFPs. In the experiment, it did not reach acceptable values ($T < 20\%$) even when UFPs were diluted 1024 times (0.00025 mol/l) because of the reactivity and physicochemical dynamics of UFPs [47] and high cyto- and genotoxicity which has been confirmed in a number of works. F. Ameen et al. [48], using soil bacteria of the genera *Rhizobium*, *Bradyrhizobium*, *Azotobacter*, *Bacillus*, *Thiobacillus*, *Pseudomonas*, *Azospirillum* and mycorrhizal fungi, pointed out the negative effects of metal UFPs, including induction of apoptosis, structural damage to the cell wall, inhibited nitrogen fixation and nitrification, suppression

of urease, N-acetylglucosaminidase, glycine aminopeptidase, arylsulfatase, polyphenol oxidase and peroxidase, which destabilize the soil community. As for manganese and cobalt itself, their toxic properties have been assessed in mammals [49, 50], plants [51-53], fish [29], invertebrates [54] and protozoans, including ciliated of rumens [26] and parasitic *Leishmania* [55]. S. Rana et al. [56], studying a consortium of algae and bacteria, identified the following stages of the impact of UFPs: changes in membrane permeability, surface adsorption, damage to transport proteins; penetration into a bacterial cell; interaction with cellular organelles; generation of reactive oxygen species (ROS); the beginning of degenerative changes. A similar effect is associated with the ability of metals exhibiting variable valence to perform lipid peroxidation and generate substances that block the active centers of enzymes [57], including luciferase which is responsible for bioluminescence [58].

However, most researchers agree that the cause of UFP toxicity is oxidative stress, leading to the production of ROS, decreased reduced glutathione levels, increased lipid peroxidation, and the release of metal ions causing protein coagulation and bacterial aggregation. Another mechanism of toxicity may be the UFPs immobilization on the cell plasmalemma, described, in particular, by T.P. Dasari et al. [59] on *E. coli* as an example. Moreover, in their work, the UFPs were arranged according to the degree of toxicity as $ZnO < CuO < Co_3O_4 < TiO_2$ in the dark and $ZnO < CuO < TiO_2 < Co_3O_4$ in the light.

Type B (competitive) means that in samples with RF without and with UFPs, the luminescence intensity was minimum at the beginning of the experiment with further growth. This dynamics can be explained based on the RF composition the main component of which is the symbiotic microbial mass. It mainly consists of bacteria, protozoa, fungi, archaea and a small proportion of phages, which are in dynamic equilibrium [60]. Essentially, this is a separate ecosystem with its own consumers and decomposers, each playing a specific role, e.g., the destruction of plant cell walls, the fermentation of organic components and the utilization of metabolic products.

Bacteria are represented mainly by anaerobic lignocellulolytic *Prevotella*, *Butyrivibrio*, *Ruminococcus*, *Lachnospiraceae*, *Ruminococcaceae*, *Bacteroidales* and *Clostridiales* [61], archaea by methanogenic *Methanobrevibacter*, *Methanosphaera* and *Methamassilicoccus* [62], fungi by *Neocallimastix*, *Caecomyces*, *Piromyces*, *Anaeromyces*, *Oorpinomyces* and *Cyllamyces* [63], ciliated and flagellated protozoa by *Entodinium* and *Epidinium* [64]. Various microorganisms secrete digestive enzymes such as cellulases, hemicellulases and ligninases. With their help, rumen microorganisms convert cellulose, hemicellulose and lignins into monosaccharides which can be further converted into volatile fatty acids, CH₄ and other products [18, 65].

Assessing the influence of the rumen fluid composition on the glow of the biosensor, E.A. Drozdova et al. [57] suggested that the reduced luminosity is due to free hydrogen ions, enzymes and ammonia in the RF. In addition, they studied the effects of glucose, propionic, lactic, succinic, acetic acid and a 10% ammonia solution. As a result, an intensification of luminescence was revealed in the first case, its slight suppression in the second-fourth cases and strong suppression in the last two cases. This is consistent with an ecological model of dynamic processes in the rumen we submit hereinbelow.

During the first minutes of the experiment, the low luminosity of the bioluminescent strain can be explained by its adaptation to the RF chemical composition and competition with anaerobic microorganisms the proportion of which will certainly decrease in air. However, fermentation processes and, as a result, the synthesis of short-chain fatty acids, ammonia, hydrogen and methane slow down. In other words, a series of negative factors that inhibit *E. coli* are excluded

while quite a lot of glucose remains in the medium. The only threat to the *E. coli* K12TG1 growth are ciliates, and the structure of the native community alters.

Similar conclusions are confirmed by our data (see Fig. 2, Table 4), therefore, it is possible to postulate an ecological model of the bioluminescence dynamics in ruminal contents (Table 6). Based on this model, the “ecooptimum” for the ratio (v/v) of the bioluminescent strain culture to diluted RF is 100 µl bacterial suspension per 100 µl of RF in a dilution of 1:64 when the luminosity of the biosensor increases throughout the test (criterion B > 1) and exceeds control values (criterion A = max).

6. Ecological model of the interaction of a Kazakh White Head Tall bull ruminal fluid with bioluminescent strain *Escherichia coli* K12TG1

Factor	Stage	Dilution																				
		1:2	1:4	1:8	1:16	1:32	1:64	1:128	1:256	1:512	1:1024	1:2048										
Negative	S																					
	F																					
Positive	S																					
	F																					
BL	S																					
	F																					
M	S																					
	F																					
A												↑	↑	↑	↑	↑	↑	con	con	↓	↓	↓
B												8.70	6.84	4.79	4.16	3.38	3.32	1.55	0.88	0.63	0.71	0.59

N a t e. Negative means negative factors (H⁺, VFA, NH₃, CH₄, predatory protozoa, competitive anaerobes), positive means nutrient substrates (including D-lucose). BL is bioluminescence intensity, A is ratio of the luminosity of the test sample to the control at the end of the test, B is ratio of luminosity at the end of the test to the beginning of the test. S (start) is beginning of the test, F (finish) is end of the test, M (movement) — dynamics of bioluminescence; — low content, — high content, — intermediate value of the component in the medium; ↓ — decrease, ↑ — increase, con — maintenance of bioluminescence at the same level.

The last test in which we studied the interaction of UFPs and RF was essentially an averaging of tests 1 and 2 with dynamic types A and B. The released metal ions react with fatty acids to form non-toxic salts, e.g., acetate, propionate, etc. They can also be bound to RF proteins and form a protein corona [37, 66] or metabolized by rumen bacteria [67] and inactivated by fungi [68]. Thereof, the initially low relative bioluminescence at high UFPs concentrations exceeded the control by the end of the experiment (see Tables 4, 5). However, there were differences between the oxides of manganese and cobalt. For the first case, the reduction and increase in luminosity occurred much faster. This may be due to the chemical nature of the elements themselves [59], the degree of their dispersity, or the possibility to form large aggregates [69] and is consistent with the data of the first experiment.

Thus, pure ultrafine particles (UFPs) of Mn₂O₃ and Co₃O₄ inhibit the luminescence of *Escherichia coli* K12TG1 in a dose-dependent manner and proportionally to the exposure time, suppressing over 50% (EC₅₀) of luminescence when diluted even 2048 times (to 0.00025 mol/l). Therefore, the toxicity index for UFPs Mn₂O₃ ranged from 89.76% at 0.25 mol/l to 38.57% at 0.00025 mol/l during the 1st minute of the exposure and from 95.16 to 52.85% at the end of the 3rd hour. For UFP Co₃O₄, these values were from 99.44 to 32.80% during the 1st minute, and from 99.43 to 54.72% at the end of the 3rd hour. Rumen fluid (RF) of a Kazakh white-headed bull, in turn, suppresses the glow only in the first minutes of exposure which may be due to the presence of “competing” anaerobic microorganisms and gradually volatilizing toxic metabolic products, e.g., ammonia. After this, RF acts as an additional nutrient substrate, intensifying luminescence by more than 7-fold at dilution 1:64. The combination of RF with particles of metal oxides leads to inhibition of their toxicity, although the maximum values of relative luminescence are still inferior to those for native rumen fluid that indicates the mutual binding of the medium components with the UFPs. Based on

the results obtained, we can argue that the ultrafine particles as sources of microelements in feeding of ruminants is promising and should be further studied..

REFERENCES

1. Mashnin D.V., Pilipchuk V.K., Avdeyuk K.S., Krasnogolovyy V.S. *Sbornik statey IV Mezhdunarodnoy nauchno-prakticheskoy konferentsii «Nauka i sovremennoe obrazovanie: aktual'nye voprosy, dostizheniya i innovatsii»* [Proc. IV Int. Conf. «Science and modern education: current issues, achievements and innovations»]. Penza, 2022: 64-66 (in Russ.).
2. Okolelova T.M., Sharipov R.I., Sharipov T.R. *Bolezni, voznikayushchie pri nepravil'nom kormlenii i soderzhanii ptitsy* [Diseases that occur due to improper feeding and keeping of poultry]. Almaty, 2018 (in Russ.).
3. Zubkova A.S., Davydova M.N., Moshkina S.V. *Materialy 70-y Mezhdunarodnoy nauchno-prakticheskoy konferentsii «Vklad universitetskoy agrarnoy nauki v innovatsionnoe razvitiye agropromyshlennogo kompleksa»* [Proc. 70 Int. Conf. «The contribution of university agricultural science to the innovative development of the agro-industrial complex»]. Ryazan', 2019: 60-63 (in Russ.).
4. Glushchenko N.N., Bogoslovskaya O.A., Baytupalov T.A., Ol'khovskaya I.P. *Mikroelementy v meditsine*, 2008, 1-2: 52 (in Russ.).
5. Ryazantseva K.V., Nechitaylo K.S., Sizova E.A. *Zhivotnovodstvo i kormoproizvodstvo*, 2021, 1: 119-137 (doi: 10.33284/2658-3135-104-1-119) (in Russ.).
6. Lyutykh O. *Effektivnoe zhivotnovodstvo*, 2020, 4(161): 95-99 (in Russ.).
7. Mishanin M.Yu., Mishanin Yu.F., Khvorostova T.V., Mishanin A.Yu. *Materialy Mezhdunarodnoy nauchno-prakticheskoy konferentsii «Sovershenstvovanie tekhnologii konservirovaniya syr'ya ras-titel'nogo i zhivotnogo proiskhozhdeniya»* [Proc. Int. Conf. «Improving the technology for canning plant and animal raw materials »]. Krasnodar, 2021: 192-196 (in Russ.).
8. Koshchaeva O.S. *Materialy I Mezhdunarodnoy nauchno-prakticheskoy konferentsii «Prioritetnye vektory razvitiya promyshlennosti i sel'skogo khozyaystva»* [Proc. I Int. Conf. «Priority vectors for the development of industry and agriculture»]. Makeevka, 2018: 100-105 (in Russ.).
9. Frolov A.N., Filippova O.B. *Vestnik Tambovskogo universiteta. Seriya: Estestvennye i tekhnicheskie nauki*, 2009, 1: 151-153 (in Russ.).
10. Gangadoo S., Stanley D., Hughes R.J., Moore R.J., Chapman J. Nanoparticles in feed: Progress and prospects in poultry research. *Trends in Food Science & Technology*, 2016, 58: 115-126 (doi: 10.1016/j.tifs.2016.10.013).
11. Kozinets A., Kozinets T., Azizbekyan S. *Zhivotnovodstvo Rossii*, 2020, 3: 35-38 (doi: 10.25701/ZZR.2019.55.61.020) (in Russ.).
12. Miroshnikov S., Sizova E., Yausheva E., Uimin M., Konev A., Minin A., Yermakov A., Nikiyan H. Comparative toxicity of CuZn nanoparticles with different physical and chemical characteristics. *Oriental Journal of Chemistry*, 2019, 3: 973 (doi: 10.13005/ojc/350308)
13. Boltianska N.I., Manita I., Podashevskaya N. Application of nanotechnology in technological processes of animal husbandry in Ukraine. *Engineering of Nature Management*, 2020, 2(16): 33-37 (doi: 10.37700/enm.2020.2(16).33-37).
14. Kumar I., Bhattacharya J. Assessment of the role of silver nanoparticles in reducing poultry mortality, risk and economic benefits. *Applied Nanoscience*, 2019, 9: 1293-1307 (doi: 10.1007/s13204-018-00942-x).
15. Rusakova E., Kosyan D., Sizova E., Miroshnikov S., Sipaylova O. Comparative evaluation of acute toxicity of nanoparticles of zinc, copper and their nanosystems using *Stylonychia mytilus*. *Oriental Journal of Chemistry*, 2015, 31(4): 105 (doi: 10.13005/ojc/31.Special-Issue1.13).
16. Kumar V., Kumari A., Guleria P., Yadav S.K. Evaluating the toxicity of selected types of nanochemicals. In: *Reviews of environmental contamination and toxicology, Vol. 215*. D. Whitacre (ed.). Springer, New York, NY, 2012: 39-121 (doi: 10.1007/978-1-4614-1463-6_2).
17. Turan N.B., Erkan H.S., Engin G.O., Bilgili M.S. Nanoparticles in the aquatic environment: Usage, properties, transformation and toxicity — a review. *Process Safety and Environmental Protection*, 2019, 130: 238-249 (doi: 10.1016/j.psep.2019.08.014).
18. Liang J., Fang W., Wang Q., Zubair M., Zhang G., Ma W., Zhang P. Metagenomic analysis of community, enzymes and metabolic pathways during corn straw fermentation with rumen microorganisms for volatile fatty acid production. *Bioresource Technology*, 2021, 342: 126004 (doi: 10.1016/j.biortech.2021.126004).
19. Nurzhanov B.S., Levakhin Yu.I., Rysaev A.F. V sbornike: *Fundamental'nye osnovy tekhnologicheskogo razvitiya sel'skogo khozyaystva: materialy rossiyskoy nauchno-prakticheskoy konferentsii s mezhdunarodnym uchastiem* [In: proceedings of the conference “Fundamental principles of agriculture technological development”]. Orenburg, 2019: 277-280 (in Russ.).
20. Aleshina E.S., Karimov I.F., Deryabin D.G. *Metody bioluminescentnogo testirovaniya: Metodicheskoe ukazaniya k laboratornomu praktikumu* [Methods of bioluminescent testing: Guidelines]. Orenburg, 2011 (in Russ.).
21. Hawco N.J., McIlvin M.M., Bundy R.M., Tagliabue A., Goepfert T.J., Moran D.M., Valentin-

- Alvarado L., DiTullio G.R., Saito M.A. Minimal cobalt metabolism in the marine cyanobacterium *Prochlorococcus*. *Proceedings of the National Academy of Sciences*, 2020, 117(27): 15740-15747 (doi: 10.1073/pnas.2001393117).
22. Bosma E.F., Rau M.H., van Gijtenbeek L.A., Siedler S. Regulation and distinct physiological roles of manganese in bacteria. *FEMS Microbiology Reviews*, 45(6): fuab028 (doi: 10.1093/femsre/fuab028).
 23. Roychoudhury A., Chakraborty S. Cobalt and molybdenum: deficiency, toxicity, and nutritional role in plant growth and development. In: *Plant nutrition and food security in the era of climate change*. V. Kumar, A.K. Srivastava, P. Suprasanna (eds.). Academic Press, 2022: 255-270 (doi: 10.1016/B978-0-12-822916-3.00021-4).
 24. Hu X., Wei X., Ling J., Chen J. Cobalt: an essential micronutrient for plant growth. *Frontiers in Plant Science*, 2021, 12: 768523 (doi: 10.3389/fpls.2021.768523).
 25. Alejandro S., Höller S., Meier B., Peiter E. Manganese in plants: from acquisition to subcellular allocation. *Frontiers in Plant Science*, 2020, 11: 300 (doi: 10.3389/fpls.2020.00300).
 26. Bonhomme A., Durand M., Quintana C., Halpern S. Influence du cobalt et de la vitamine B12 sur la croissance et la survie des ciliés du rumen in vitro, en fonction de la population bactérienne. *Reproduction Nutrition Développement*, 1982, 22(1A): 107-122 (doi: 10.1051/rnd:19820109).
 27. Hai Y., Dugery R.J., Healy D., Christianson D.W. Formiminoglutamase from *Trypanosoma cruzi* is an arginase-like manganese metalloenzyme. *Biochemistry*, 2013, 52(51): 9294-9309 (doi: 10.1021/bi401352h).
 28. Li A.-H., Na B.-K., Song K.-J., Lim S.-B., Chong C.-K., Park Y.-K., Kim T.-S. Identification and characterization of a mitochondrial manganese superoxide dismutase of *Spirometra erinacei*. *Journal of Parasitology*, 2011, 97(6): 1106-1112 (doi: 10.1645/GE-2753.1).
 29. Nechev J., Stefanov K., Popov S. Effect of cobalt ions on lipid and sterol metabolism in the marine invertebrates *Mytilus galloprovincialis* and *Actinia equine*. *Comparative Biochemistry and Physiology Part A: Molecular & Integrative Physiology*, 2006, 144(1): 112-118 (doi: 10.1016/j.cbpa.2006.02.022).
 30. Tajchman K., Ukalska-Jaruga A., Bogdaszewski M., Pecio M., Janiszewski P. Comparison of the accumulation of macro- and microelements in the bone marrow and bone of wild and farmed red deer (*Cervus elaphus*). *BMC Veterinary Research*, 2021, 17(1): 1-11 (doi: 10.1186/s12917-021-03041-2).
 31. Liu Y., Zhang J., Wang C., Liu Q., Guo G., Huo W., Chen L., Zhang Y., C. Pei C., Zhang S. Effects of folic acid and cobalt sulphate supplementation on growth performance, nutrient digestion, rumen fermentation and blood metabolites in Holstein calves. *British Journal of Nutrition*, 2022, 127(9): 1313-1319 (doi: 10.1017/S000711452100221X).
 32. Archibald F.S., Fridovich I. The scavenging of superoxide radical by manganous complexes: in vitro. *Archives of Biochemistry and Biophysics*, 1982, 214(2): 452-463 (doi: 10.1016/0003-9861(82)90049-2).
 33. Barnese K., Gralla E.B., Valentine J.S., Cabelli D.E. Biologically relevant mechanism for catalytic superoxide removal by simple manganese compounds. *Proceedings of the National Academy of Sciences*, 2012, 109(18): 6892-6897 (doi: 10.1073/pnas.1203051109).
 34. Anjem A., Imlay J.A. Mononuclear iron enzymes are primary targets of hydrogen peroxide stress. *Journal of Biological Chemistry*, 2012, 287(19): 15544-15556 (doi: 10.1074/jbc.M111.330365).
 35. Sobota J.M., Imlay J.A. Iron enzyme ribulose-5-phosphate 3-epimerase in *Escherichia coli* is rapidly damaged by hydrogen peroxide but can be protected by manganese. *Proceedings of the National Academy of Sciences*, 2011, 108(13): 5402-5407 (doi: 10.1073/pnas.1100410108).
 36. Zeinert R., Martinez E., Schmitz J., Senn K., Usman B., Anantharaman V., Aravind L., Waters L.S. Structure—function analysis of manganese exporter proteins across bacteria. *Journal of Biological Chemistry*, 2018, 293(15): 5715-5730 (doi: 10.1074/jbc.M117.790717).
 37. Waters L.S. Bacterial manganese sensing and homeostasis. *Current Opinion in Chemical Biology*, 2020, 55: 96-102 (doi: 10.1016/j.cbpa.2020.01.003).
 38. Smith A.D., Warren M.J., Refsum H. Vitamin B12. *Advances in Food and Nutrition Research*, 2018, 83: 215-279 (doi: 10.1016/bs.afnr.2017.11.005).
 39. Erikson K.M., Aschner M. Manganese: its role in disease and health. In: *Essential metals in medicine: therapeutic use and toxicity of metal ions in the clinic*. P.L. Carver (ed.). De Gruyter, Berlin, Boston, 2019: 253-266 (doi: 10.1515/9783110527872-010).
 40. Balachandran R.C., Mukhopadhyay S., McBride D., Veevers J., Harrison F.E., Aschner M., Haynes E.N., Bowman A.B. Brain manganese and the balance between essential roles and neurotoxicity. *Journal of Biological Chemistry*, 2020, 295(19): 6312-6329 (doi: 10.1074/jbc.REV119.009453).
 41. Martins Jr. A.C., Gubert P., Villas Boas G.R., Meirelles Paes M., Santamaría A., Lee E., Tinkov A.A., Bowman A.B., Aschner M. Manganese-induced neurodegenerative diseases and possible therapeutic approaches. *Expert Review of Neurotherapeutics*, 2020, 20(11): 1109-1121 (doi: 10.1080/14737175.2020.1807330).
 42. Warren M.J., Raux E., Schubert H.L., Escalante-Semerena J.C. The biosynthesis of adenosylcobalamin (vitamin B12). *Natural Product Reports*, 2002, 19(4): 390-412 (doi: 10.1039/b108967f).
 43. Osman D., Cooke A., Young T.R., Deery E., Robinson N.J., Warren M.J. The requirement for

- cobalt in vitamin B₁₂: a paradigm for protein metalation. *Biochimica et Biophysica Acta (BBA)-Molecular Cell Research*, 2021, 1868(1), 118896 (doi: 10.1016/j.bbamcr.2020.118896).
44. Tjong E., Dimri M., Mohiuddin S.S. *Biochemistry, Tetrahydrofolate*. StatPearls Publishing, 2021.
 45. Budinger D., Barral S., Soo A.K., Kurian M.A. The role of manganese dysregulation in neurological disease: emerging evidence. *The Lancet Neurology*, 2021, 20(11): 956-968 (doi: 10.1016/S1474-4422(21)00238-6).
 46. Lison D., Van Den Brûle S., Van Maele-Fabry G. Cobalt and its compounds: update on genotoxic and carcinogenic activities. *Critical Reviews in Toxicology*, 2018, 48(7): 522-539 (doi: 10.1080/10408444.2018.1491023).
 47. Mauter M.S., Zucker I., Perreault F., Werber J.R., Kim J.H., Elimelech M. The role of nanotechnology in tackling global water challenges. *Nature Sustainability*, 2018, 1(4): 166-175 (doi: 10.1038/s41893-018-0046-8).
 48. Ameen F., Alsamhary K., Alabdullatif J.A., ALNadhari S. A review on metal-based nanoparticles and their toxicity to beneficial soil bacteria and fungi. *Ecotoxicology and Environmental Safety*, 2021, 213: 112027 (doi: 10.1016/j.ecoenv.2021.112027).
 49. Danzeisen R., Weight D., Blakeney M., Boyle D. A tiered approach to investigate the inhalation toxicity of cobalt substances. Introduction: Cobalt's essential role in nature and technology. *Regulatory Toxicology and Pharmacology*, 2022, 130: 105125 (doi: 10.1016/j.yrtph.2022.105125).
 50. Leyssens L., Vinck B., Van Der Straeten C., Wuyts F., Maes L. Cobalt toxicity in humans — a review of the potential sources and systemic health effects. *Toxicology*, 2017, 387: 43-56 (doi: 10.1016/j.tox.2017.05.015).
 51. Yang S., Ling G., Li Q., Yi K., Tang X., Zhang M., Li X. Manganese toxicity-induced chlorosis in sugarcane seedlings involves inhibition of chlorophyll biosynthesis. *The Crop Journal*, 2022, 10(6): 1674-1682 (doi: 10.1016/j.cj.2022.04.008).
 52. Noor I., Sohail H., Hasanuzzaman M., Hussain S., Li G., Liu J. Phosphorus confers tolerance against manganese toxicity in *Prunus persica* by reducing oxidative stress and improving chloroplast ultrastructure. *Chemosphere*, 2022, 291(part 3): 132999 (doi: 10.1016/j.chemosphere.2021.132999).
 53. Tang T., Tao F., Li W. Characterisation of manganese toxicity tolerance in *Arabidopsis paniculata*. *Plant Diversity*, 2021, 43(2): 163-172 (doi: 10.1016/j.pld.2020.07.002).
 54. Ali Z., Yousafzai A.M., Sher N., Muhammad I., Nayab G.E., Aqeel S.A.M., Shah S.T., Aschner M., Khan I., Khan H. Toxicity and bioaccumulation of manganese and chromium in different organs of common carp (*Cyprinus carpio*) fish. *Toxicology Reports*, 2021, 8: 343-348 (doi: 10.1016/j.toxrep.2021.02.003).
 55. Tavakoli P., Ghaffarifar F., Delavari H., Shahpari N. Efficacy of manganese oxide (Mn₂O₃) nanoparticles against *Leishmania major* in vitro and in vivo. *Journal of Trace Elements in Medicine and Biology*, 2019, 56: 162-168 (doi: 10.1016/j.jtemb.2019.08.003).
 56. Rana S., Kumar A. Toxicity of nanoparticles to algae-bacterial co-culture: knowns and unknowns. *Algal Research*, 2022, 62: 102641 (doi: 10.1016/j.algal.2022.102641).
 57. Drozdova E.A., Karimov I.F. *Vestnik Orenburgskogo gosudarstvennogo universiteta*, 2014, 6(167): 104-107 (in Russ.).
 58. Liu Y.-J. Understanding the complete bioluminescence cycle from a multiscale computational perspective: a review. *Journal of Photochemistry and Photobiology C: Photochemistry Reviews*, 2022, 52: 100537 (doi: 10.1016/j.jphotochemrev.2022.100537).
 59. Dasari T.P., Pathakoti K., Hwang H.M. Determination of the mechanism of photoinduced toxicity of selected metal oxide nanoparticles (ZnO, CuO, Co₃O₄ and TiO₂) to *E. coli* bacteria. *Journal of Environmental Sciences*, 2013, 25(5): 882-888 (doi: 10.1016/S1001-0742(12)60152-1).
 60. Weimer P.J. Redundancy, resilience, and host specificity of the ruminal microbiota: implications for engineering improved ruminal fermentations. *Frontiers in Microbiology*, 2015, 6: 296 (doi: 10.3389/fmicb.2015.00296).
 61. Henderson G., Cox F., Ganesh S., Jonker A., Young W., Global Rumen Census Collaborators, Janssen P.H. Rumen microbial community composition varies with diet and host, but a core microbiome is found across a wide geographical range. *Scientific Reports*, 2015, 5(1): 14567 (doi: 10.1038/srep14567).
 62. Lan W., Yang C. Ruminant methane production: Associated microorganisms and the potential of applying hydrogen-utilizing bacteria for mitigation. *Science of the Total Environment*, 2019, 654: 1270-1283 (doi: 10.1016/j.scitotenv.2018.11.180).
 63. Fliegerova K., Kaerger K., Kirk P., Voigt K. Rumen fungi. In: *Rumen microbiology: from evolution to revolution*. A. Puniya, R. Singh, D. Kamra (eds.). Springer, New Delhi, 2015: 97-112 (doi: 10.1007/978-81-322-2401-3_7).
 64. Newbold C.J., De la Fuente G., Belanche A., Ramos-Morales E., McEwan N.R. The role of ciliate protozoa in the rumen. *Frontiers in Microbiology*, 2015, 6: 1313 (doi: 10.3389/fmicb.2015.01313).
 65. Liang J., Nabi M., Zhang P., Zhang G., Cai Y., Wang Q., Ding Y. Promising biological conversion of lignocellulosic biomass to renewable energy with rumen microorganisms: A comprehensive review. *Renewable and Sustainable Energy Reviews*, 2020, 134: 110335 (doi: 10.1016/j.rser.2020.110335).
 66. Saptarshi S.R., Duschl A., Lopata A.L. Interaction of nanoparticles with proteins: relation to bio-reactivity of the nanoparticle. *Journal of Nanobiotechnology*, 2013, 11(1): 26 (doi: 10.1186/1477-3155-11-26).

67. Spagnoletti F.N., Kronberg F., Spedalieri C., Munarriz E., Giacometti R. Protein corona on biogenic silver nanoparticles provides higher stability and protects cells from toxicity in comparison to chemical nanoparticles. *Journal of Environmental Management*, 2021, 297: 113434 (doi: 10.1016/j.jenvman.2021.113434).
68. Galindo T.P.S., Pereira R., Freitas A.C., Santos-Rocha T.A.P., Rasteiro M.G., Antunes F., Rodrigues D., Soares A.M.V.M., Gonçalves F., Duarte A.C., Lopes I. Toxicity of organic and inorganic nanoparticles to four species of white-rot fungi. *Science of the Total Environment*, 2013, 458-460: 290-297 (doi: 10.1016/j.scitotenv.2013.04.019).
69. Parsai T., Kumar A. Effect of seawater acidification and plasticizer (Bisphenol-A) on aggregation of nanoparticles. *Environmental Research*, 2021, 201: 111498 (doi: 10.1016/j.envres.2021.111498).